

Wavefront splitting intrinsic Fabry-Perot fiber optic sensor

Zhengyu Huang
Xiaopei Chen
Yizheng Zhu
Anbo Wang

Virginia Polytechnic Institute and State University
Center for Photonics Technology
Department of Electrical and Computer Engineering
Blacksburg, Virginia 24061-0111

Abstract. We present the principle, fabrication, and characterization of a novel wavefront splitting intrinsic Fabry-Perot fiber temperature sensor. The sensor is made by splicing a section of fused silica tubing to the tip of a single-mode fiber. The completed sensor has the same diameter as the fiber and the sensor length is less than 0.5 mm. © 2005 Society of Photo-Optical Instrumentation Engineers.
[DOI: 10.1117/1.1978847]

Subject terms: fiber sensors; Fabry-Perot; splice.

Paper L040815RR received Nov. 29, 2004; revised manuscript received Apr. 26, 2005; accepted for publication May 16, 2005; published online Jul. 22, 2005.

1 Introduction

Intrinsic Fabry-Perot interferometer (IFPI) fiber sensors are well known for their ability to measure temperature, strain, pressure, and ultrasound perturbations due to their excellent sensitivity, rapid response, immunity to electromagnetic interference, and potential of multiplexing.¹

The interferometers can be divided into two major categories: amplitude splitting interferometers and wavefront splitting interferometers.² Most of the IFPI sensors are based on the amplitude splitting principle. The amplitude splitting scheme varies from using different mode-field-diameter single-mode fibers, internal mirrors to fiber micro cavities,^{1,3-5} to name just a few. However, fiber polishing,¹ dielectric mirror deposition, and arc splicing³ impose stringent control in the sensor fabrication.

We report here an IFPI fiber sensor that is based on a wavefront splitting principle. Only splicing and cleaving of a section of fused silica tubing to the single-mode fiber (SMF) is used. The fabrication process is significantly simplified and equivalent performance to the traditional IFPI sensor is achieved. The theoretical analysis, sensor fabrication, as well as sensor performance are presented.

2 Principles of Operation

The wavefront split IFPI structure is illustrated in Fig. 1. A piece of fused silica tubing is spliced to the SMF, and then cleaved close to the splice point. The wavefront of the guiding LP₀₁ mode of the SMF is split into two components at the fiber-tubing interface. The two components are reflected by the fiber core-air interface and cleaved tubing end, respectively. The Fabry-Perot cavity length is the optical length of the fused silica tubing. The interference spectrum is obtained by a sensor interrogator, and the cavity length is calculated by a high-precision white-light algorithm.⁶

The reflectivity R is given by the Fresnel formula²

$$R = \left(\frac{n_{\text{glass}} - n_{\text{air}}}{n_{\text{glass}} + n_{\text{air}}} \right)^2 \quad (1)$$

where n_{glass} and n_{air} are refractive indices of fused silica and air.

The electric fields from the cleaved SMF reflection, fiber core-air reflection, and fused silica tubing reflection are shown in Fig. 1 and given by

$$E_R(r, \varphi) = A_0 \sqrt{R} e^{-\frac{r^2}{w^2}} \quad (2)$$

$$E_{\text{core}}(r, \varphi) = \begin{cases} E_R(r, \varphi), & r \leq a \\ 0, & r > a \end{cases} \quad \text{and} \quad (3)$$

$$E_{\text{tube}}(r, \varphi) = \begin{cases} E_R(r, \varphi), & r \geq a \\ 0, & r < a \end{cases}$$

where A_0 is the magnitude of the incident electric field, w is the mode-field radius of the single-mode fiber, and a is the inner radius of the fused silica tube. Gaussian field distribution approximation⁷ is used in Eq. (2).

Only those of the truncated reflection components coupled into the fundamental mode of the SMF can reach the detector. The coupling coefficients are

$$\eta_{\text{core}} = \frac{\int_0^{2\pi} \int_0^a E_{\text{core}} E_R^* r \, dr \, d\varphi}{\int_0^{2\pi} \int_0^{+\infty} E_R E_R^* r \, dr \, d\varphi} \quad \text{and} \quad (4)$$

$$\eta_{\text{tube}} = \frac{\int_0^{2\pi} \int_a^{+\infty} E_{\text{tube}} E_R^* r \, dr \, d\varphi}{\int_0^{2\pi} \int_0^{+\infty} E_R E_R^* r \, dr \, d\varphi}$$

Thus the normalized reflection power of the two components is given by η^2 .

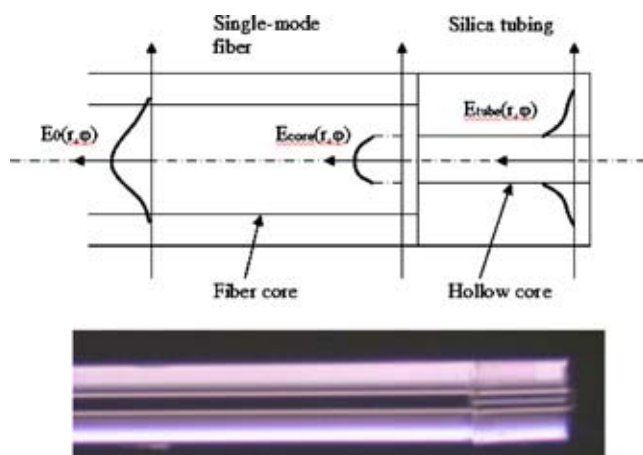


Fig. 1 Split wavefront IFPI sensor head structure.

3 Sensor Fabrication

The objective of IFPI fabrication is to obtain large signal-to-noise ratio and high fringe visibility. In the fabrication process, the fused silica tubing is first spliced to an SMF. The fiber tubing is then put on a fiber cleaver and placed under a microscope. The splicing point can be easily identified under the microscope. The tubing is then cleaved at a distance to the splicing point. Corning SMF28 and fused silica tubing from Polymicro Technologies are used. The fiber splicer and cleaver used are Type-36 Fiber Splicer (Sumitomo Electric) and CT-04B High Precision Fiber Cleaver (Fujikura). The microscope is from Olympus (SZ40). A Si720 system (Micron Optics) is used as sensor interrogator.

It is found that fiber core-air reflection decreases monochromatically when increasing either the fusion splicing arc power or the arc duration as shown in Fig. 2 (the arc power P and arc duration D are normalized to $P=15$ and $D=2.0$, which is used in the standard SMF splicing configuration). This is because the silica tubing inner diameter shrinks with the increasing amount of arc generated heat, which results in a decreased effective reflection area. Therefore to fabricate a good IFPI sensor, low arc power and short arc duration that does not degrade the mechanical strength of the sensor is adopted. Silica tubing with a $5\text{-}\mu\text{m}$ inner diameter is chosen because it provides the closest magnitudes of reflections on both interfaces, therefore high fringe visibility. The experimental data is compared with theoretical prediction in Fig. 3, which proves the coupling model a valid assumption. The tubing should be well cleaved, because a tilted end face will increase the coupling loss of the reflection to the single-mode fiber and reduce the fringe visibility. The silica tubing length should be controlled within a $500\text{-}\mu\text{m}$ range. The light in the tubing will diverge because it is no longer confined in a waveguide structure. Longer cavity length would result in larger divergence and less reflected light coupled into the single-mode fiber.

Since the fiber splicing process is highly repeatable and controlling the IFPI length within $500\ \mu\text{m}$ is not difficult

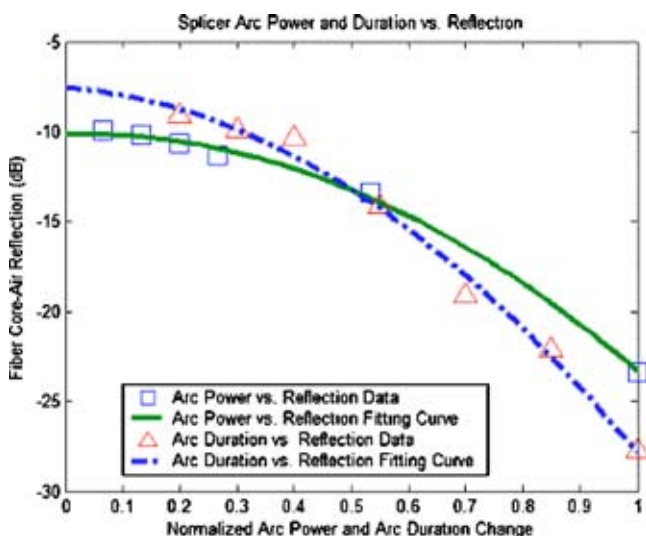


Fig. 2 IFPI fiber core-air reflection vs splicing arc power and duration (normalized to cleaved SMF reflection).

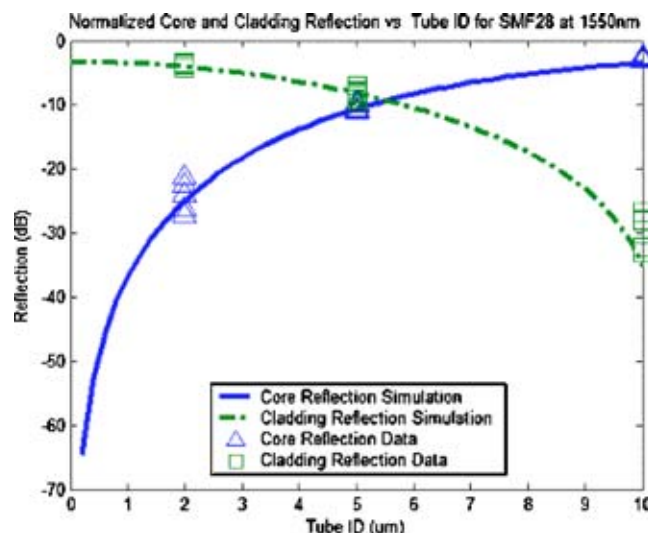


Fig. 3 IFPI core and cladding reflection (normalized to cleaved SMF reflection).

with a microscope, the chance of successful IFPI fabrication is only dependent on the cleaving quality of the tube. Ten out of 13 sensors that we have made demonstrate over 10-dB peak-to-peak fringe as shown in Fig. 4. With a fine-tuned fiber cleaver, the successful rate of IFPI fabrication is expected to exceed 75%.

4 Sensor Performance

The sensor is co-positioned with a thermocouple (K-type, Omega) in a double-bore ceramic tube and then placed in a furnace (Thermolyne 48000). The function of the ceramic tube is to dampen the temperature fluctuation. The temperature is increased with 50°C per step and 1 h at each step from room temperature to 600°C back to room temperature for four cycles. The mean value of sensor's optical path difference (OPD) at each temperature step is shown in Fig. 4. The maximum deviation between the experimental OPD curve and the four-time averaged OPD curve is $\pm 0.23\ \text{nm}$.

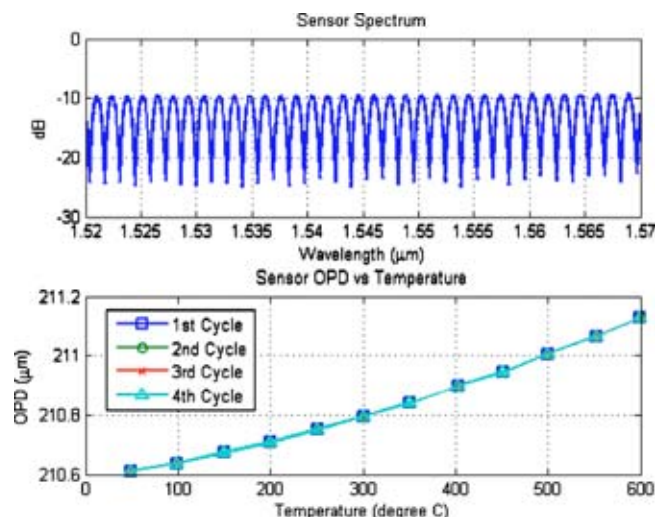


Fig. 4 IFPI spectrum and temperature performance (normalized to cleaved SMF reflection).

The total OPD change from 50°C to 600°C is 517.0 nm. Thus the sensor repeatability is approximately $\pm 0.24^\circ\text{C}$ and $\pm 0.046\%$ of the dynamic range. The resolution of the sensor system is usually interpreted by its standard deviation of temperature measurements. It is common to use twice the standard deviation (STD) as the direct measure of resolution. The sensor is inserted into a ceramic tube and placed in an environmental chamber (Test Equity 1000 Series Temperature Chamber) at 25°C for 5 h, and the OPD is sampled every 5 s. The STD is 0.13 nm. The resolution of the sensor system is 0.26 nm, which corresponds to 0.27°C and 0.05% of its dynamic range. The nonlinear behavior of the sensor is caused by the temperature sensitivity of both the refractive index of silica glass and the length of the cavity.

5 Conclusion

In this letter, we presented the principle of the proposed wavefront splitting IFPI followed by discussion on fabrication optimization. The IFPI is made with a 5- μm ID fused

silica tube. Short arc duration and low arc power is used in the sensor fabrication. The sensor is measured to 600°C for four cycles and demonstrated 0.27°C resolution and $\pm 0.24^\circ\text{C}$ repeatability.

References

1. W.-H. Tsai and C.-J. Lin, "A novel structure for the intrinsic Fabry-Perot fiber-optic temperature sensor," *J. Lightwave Technol.* **19**(5), 682–686 (May 2001).
2. M. Born and E. Wolf, *Principles of Optics*, Cambridge University Press, 7th ed., Cambridge, UK (1999).
3. C. E. Lee, W. N. Gibler, R. A. Atkins, and H. F. Taylor, "In-line fiber Fabry-Perot interferometer with high-reflectance internal mirrors," *J. Lightwave Technol.* **10**(10), 1376–1379 (Oct. 1992).
4. Y. L. Lo, J. S. Sirkis, and C. C. Chang, "Passive signal processing of in-line fiber etalon sensor for high strain-rate loading," *J. Lightwave Technol.* **15**(8), 1578–1586 (1997).
5. H. Singh and J. S. Sirkis, "Simultaneously measuring temperature and strain using optical fiber microcavities," *J. Lightwave Technol.* **15**(4), 647–653 (1997).
6. Q. Bing, G. Pickrell, J. Xu, Z. Huang, et al., "Novel data processing techniques for dispersive white light interferometer," *Opt. Eng.* **43**(11), 3165–3171 (2003).
7. D. Marcuse, "Loss analysis of single-mode fiber splices," *Bell Syst. Tech. J.* **56**(5), 703–718 (1977).